Impact of Microcracks on the Performance of a Crystalline Silicon Photovoltaic Cell

Dibyendu Hazra[1], Roopmati Meena[1], Ravi Kumar[1], and Rajesh Gupta[1]

[1]Department of Energy Science and Engineering

Indian Institute of Technology Bombay, Mumbai (India)

Abstract

Solar cells are susceptible to the formation of microcracks throughout different stages of their lifespan. Microcracks can lead to power loss through different impacting mechanisms, such as enhancing surface recombination or increasing resistive losses, leading to performance loss in solar cells. These operating mechanisms can co-occur in a solar cell, which has yet to be studied in detail. In this work, the impact of different operating mechanisms of microcracks on the electrical performance of a solar cell has been analysed using PSpice simulations. Three scenarios have been considered to assess the effects of microcracks, namely, enhanced surface recombination mode, resistive loss mode, and a combination of both. Simulations have been performed using a distributed diode model of the solar cell for the three most occurring microcrack orientations. The results show that in resistive mode, the power loss is comparatively less for all microcrack orientations. For parallel to busbar microcrack, no resistive power loss is observed, and for diagonal and perpendicular to busbar microcrack, after a certain threshold resistance, the power loss does not increase due to changes in the path of the lateral current flow. The recombinative loss mode results in higher performance loss than the resistive loss mode. Further, depending on the presence of stress factors, performance loss due to a combination of both loss modes leads to higher performance loss, impacting its reliability. This work highlights the possible extent of performance loss due to the different operating mechanisms of microcracks.

Keywords: Microcracks, Recombinations, Resistive loss, Solar cell, Photovoltaics, Power loss

1. Introduction

In the modern world, most of our current power consumption is supplied using fossil fuels, which are non-renewable and not environmentally friendly. Shifting to renewable energy resources like solar, wind, and hydro is necessary to meet the future energy needs of the growing population. Out of the available renewable energy sources, the photovoltaic (PV) industry has developed into one of the fastest-growing technologies in recent decades. This is mainly because the PV modules generally have a comparatively higher lifetime, lower long-term costs and local as well as grid-level energy generation capability. In the last decade, the weighted average of the levelized cost of electricity for commercial-scale solar PV has dropped from 0.381 USD/kWh to 0.057 USD/kWh (IRENA Renewable Cost Database, 2020), making solar energy the most cost-efficient and viable energy source right now. Crystalline silicon (c-Si) PV modules currently dominate the PV market industry due to being the most abundant and well-researched. PV modules operate under harsh environmental conditions, resulting in defects and degradations, significantly impacting the performance of PV modules in the long term. International Technology Roadmap for Photovoltaics (ITRPV) reported a significant reduction in the wafer thickness of solar cells to reduce the cost (ITRPV, 2018). However, thinner wafers lowered the robustness of the solar cell against thermo-mechanical loads, resulting in a higher chance of cell cracking. Microcracks in solar cells are one of the critical forms of defect and degradation in crystalline silicon solar cells, which can propagate, resulting in increased severity and leading to other degradation modes. Microcracks can form due to thermo-mechanical stress in the cells during manufacturing, transportation, and outdoor operating conditions due to temperature variation, hailstorms, snow, wind, etc. Microcracks are invisible to the bare eye as they have a width of less than 30μm (Dhimish *et al.*, 2017). They can be detected through imaging processes such as electroluminescence (EL) imaging. Herein, microcracks appear as dark lines due to reduced EL emission caused by carrier recombination sites created around the microcrack region (Mohammed Niyaz, Meena and

10.18086/swc.2023.01.02 Available at http://proceedings.ises.org

Gupta, 2021). Microcracks do not electrically disconnect cell areas; however, they can interrupt fingers along the length of the microcrack, increasing the series resistance. Dhimish et al. have reported a power loss of up to 20% due to microcracks at the module level (Dhimish *et al.*, 2017). In addition to resistive losses, microcracks may also lead to an increase in surface recombination (Buerhop *et al.*, 2012). Herein, the severity and area of surface recombination vary with the length, width, depth and orientation of the microcracks (Buerhop *et al.*, 2012; Papargyri *et al.*, 2020; Mohammed Niyaz, Meena and Gupta, 2021). While each of the aforementioned loss-incurring modes of microcrack has been studied in isolation, they may co-occur under outdoor field conditions, which needs to be studied further. In this work, the impact of microcracks based on their operating mechanism on electrical performance has been investigated at the cell level using a simulation approach. For the simulations, the distributed diode model of solar cells has been used, where the microcracks are modelled with local parameter variation depending on the position of the microcracks. Diagonal, perpendicular to the busbar and parallel to the busbar orientations of microcracks and three power loss incurring mechanisms due to microcracks have been considered for the simulations.

The further sections of this article are structured as follows. Section 2 describes the three different electrical models used for solar cell modelling. Section 3 depicts the detailed model used in the modelling of microcracks in this paper. In section 4, the simulation results have been discussed, and finally, section 5 concludes this paper.

2. Electrical modelling of solar cells

The modelling and simulation approach is helpful in studying the effects of change in parameters due to microcracks in a solar cell, which is difficult to change experimentally. There are several electrical models for solar cells to accommodate different needs in modelling certain phenomena. The different electrical models for solar are discussed in the following sections.

2.1. Single-diode model of solar cell

The solar cell can be represented by an equivalent circuit using the single diode model (SDM) shown in Fig. 1. In this model, the current source, J_L, represents the light-generated current density due to the illumination of the solar cell. The diode represents the p-n junction in the solar cell. R_S is the series resistance due to a combination of base-emitter and contact resistance between metals and silicon. R_{sh} is the shunt leakage resistance typically due to manufacturing defects.

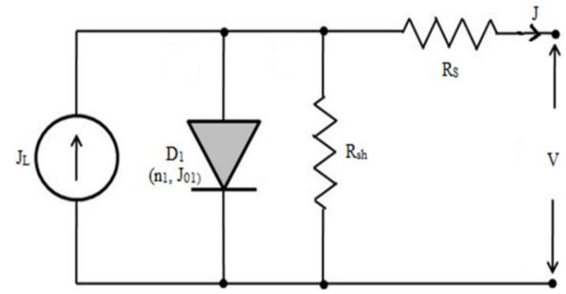

Fig. 1: Solar cell equivalent circuit using single diode model

The current-voltage (*I-V*) characteristics equation of this solar cell equivalent circuit can be written as

$$J = J_L - J_0\{exp[\frac{q(V+JR_S)}{n_1kT}] - 1\} - \frac{V+JR_S}{R_{sh}} \quad \text{(eq. 1)}$$

Here, n_1 is called the ideality factor, K is the Boltzmann constant, and T is the absolute temperature of the solar cell. In a single-diode model, the value for the ideality factor is taken as constant. In operating conditions, the ideality factor varies as a function of the applied voltage across the solar cell (Kikelj *et al.*, 2021). The ideality factor is close to one when the surface and bulk regions dominate the recombinations in the solar cell. However, when the recombination around the p-n junction dominates, the ideality factor approaches two. To model the junction recombinations, the double diode model is used.

2.2. Double-diode model of solar cell

In the double diode model, a second diode representing junction recombination is added in parallel with the first one. Typically, the ideality factor of the diode is taken as two. The circuit of the double diode model is shown in Fig. 2.

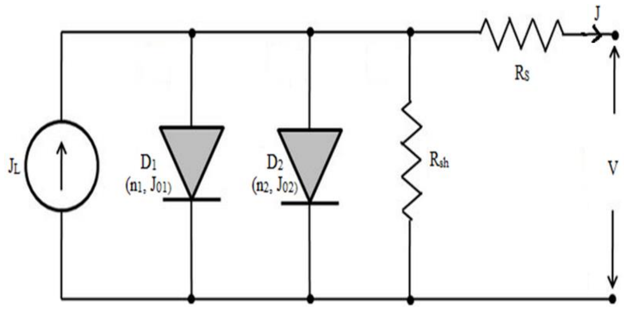

Fig. 2: Double diode model of solar cell

J_L is the light-generated current density, D_1 ($n_1 = 1$, J_{01}) represents the bulk recombination and, D_2 ($n_2 = 2$, J_{02}) represents recombination in the junction, R_s and R_{sh} represent the series resistance and shunt resistance of the solar cell, respectively. The mathematical expression for the double diode model's output current density (J) can be written as given in eq. 2 (PVEducation).

$$J = J_L - J_{01}\{exp[\frac{q(V+JR_S)}{kT}] - 1\} - J_{02}\{exp[\frac{q(V+JR_S)}{2kT}] - 1\} - \frac{V+JR_S}{R_{sh}} \quad \text{(eq. 2)}$$

2.3. Distributed diode model of solar cell

In single and double-diode models, the complete solar cell is taken as a whole and considers uniform effects of all parameters. In reality, there is a non-uniform current generation being different in sites of finger, busbar and emitter sheet. Also, due to the lateral flow of current on the surface of the cell, there is a voltage drop across the length (Zekry and Al-Mazroo, 1996). To consider these effects and the spatial non-uniformity of the solar cell, a 3D model called the distributed diode model is used (Spataru *et al.*, 2015). In the distributed diode model, the solar cell is divided into several small elemental areas, which are modelled by the single or double diode model. Each elemental area consists of a diode, a shunt resistance and a current source connected in parallel. Each neighbouring elementary area is connected with a series resistance. Using this model, anomalies in small parts of the solar cell can be detected easily due to modelling such small elemental areas.

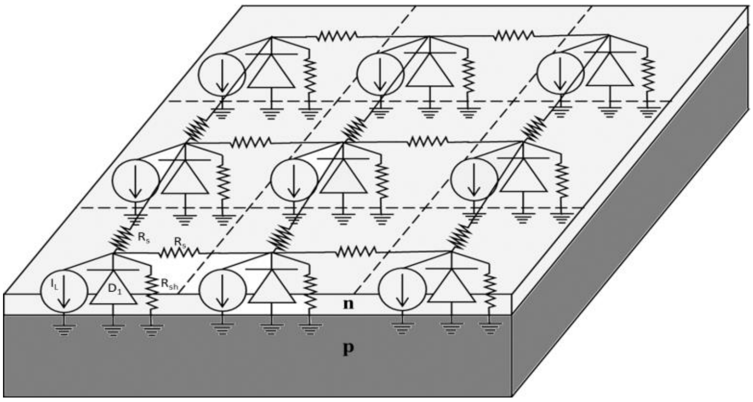

Fig. 3: Distributed diode model approach of solar cells

In Fig. 3, a simple 3x3 distributed diode model is shown, which is extended further in all directions in 3-D to model an entire solar cell. In this work, the distributed diode model has been used to model the microcracks in solar cells. The model used is discussed in the next section.

3. Modelling of microcracks

In the current work, microcracks have been modelled and analyzed for their impact on the performance of solar cells. Microcracks can affect the solar cell parameters in a few ways. An air gap is created on the surface of the cell along the length of the microcrack due to the width and depth of a microcrack. The air gap hinders lateral current flow on the surface, thus increasing the emitter resistance. Recombination sites form on the microcrack location due to dangling bonds. Also, due to higher resistance across the microcrack, the charge carriers are blocked. The blocked charge carriers at the edge of the microcracks increase the recombination around the p-n junction along the microcrack (Van Mölken *et al.*, 2012; Kasewieter *et al.*, 2014). Also, short-circuit paths can form in microcrack locations due to the shorting of the p-n junction due to other material defects around the microcrack location, increasing the shunt resistance. Microcrack and shunt area due to microcrack are directly related, and shunt area increases with the microcrack's length, width and depth (Buerhop *et al.*, 2012; Demant *et al.*, 2016; Dong *et al.*, 2018). These different physical phenomenon affects different solar cell parameters, thus impacting the performance of the solar cell.

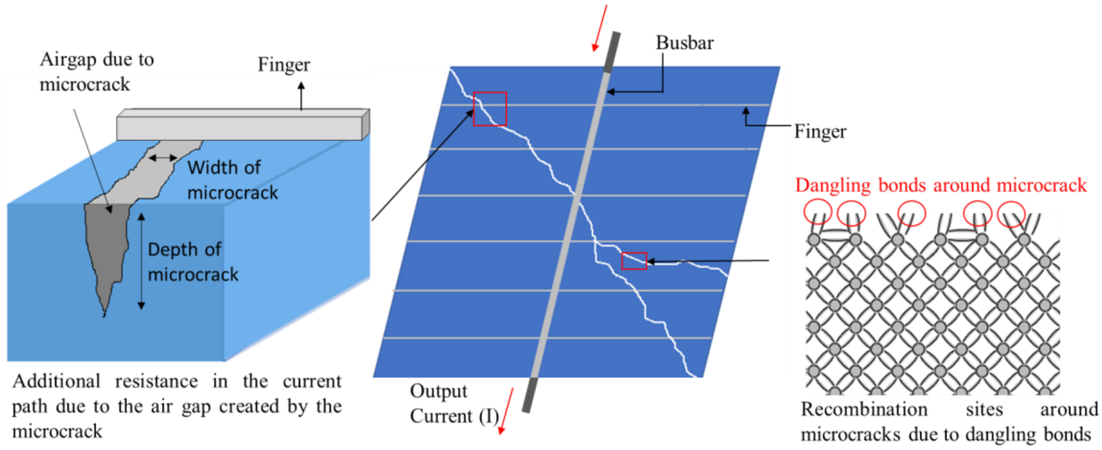

Fig. 4: Schematic of different impact mechanisms of microcrack

In the current study, the spatial characteristics of microcracks have been modelled using the distributed diode model of solar cells. In this model, a grid of 100×100 smaller sub-cells have been created by dividing a healthy solar cell with three busbars. Each sub-cell is modelled using essentially the two-diode model using the combination of a current source (I_L), two diodes (D_1, D_2), and a shunt resistance (R_{sh}) to represent the p-n junction in the solar cell, as illustrated in Fig. 5(a). Distinct sub-cells (as depicted in Fig. 5(b)) are linked through resistive elements such as sheet resistance (R_{sheet}), finger resistance (R_{finger}), and busbar resistance (R_{busbar}), depending on the sub-cell's spatial location. A standard 15.6 cm x 15.6 cm cell is considered for the model, and it is simulated in the PSpice circuit simulator.

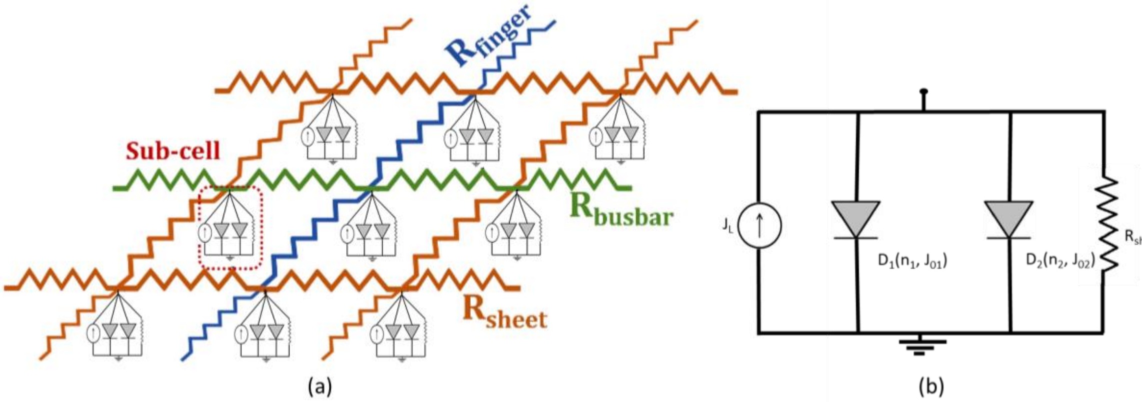

Fig. 5 (a) Distributed diode model using different sub-cells (b) Individual sub-cell

The parameters that are used in the simulations using the above model are depicted in Tab. 1. The parameter values here represent a healthy solar cell. The numerical values for the simulation are taken from Meena et al., where the values have been experimentally obtained (Meena, Niyaz and Gupta, 2023).

Value for each sub-cell is calculated the following way,

$$I_{sc}(\text{node}) = \frac{I_{sc}(\text{experiment})}{Number\ of\ active\ nodes\ in\ the\ circuit} \quad \text{(eq. 3)}$$

$$I_0(\text{node}) = \frac{I_0(\text{experiment})}{\text{Total number of nodes in the circuit}} \quad \text{(eq. 4)}$$

$$R_{sh}(\text{node}) = R_{sh}(\text{experiment}) \times \text{Total number of nodes in the circuit} \quad \text{(eq. 5)}$$

Tab. 1: Numerical values of different components used in the distributed diode model

Parameter	Value
I_{sc} (A/node)	1.0996×10^{-3}
n_1	1
n_2	2
J_{01} (A/cm^2)	1×10^{-11}
J_{02} (A/cm^2)	1×10^{-9}
R_{sh} (Ω/node)	3.603×10^{5}
R_{sheet} (Ω/cm)	90
R_{finger} (Ω/cm)	2.89×10^{-4}
R_{busbar} (Ω/cm)	2.58×10^{-5}

The resistive components (R_{sheet}, R_{finger}, R_{busbar}) are obtained from the literature Meena et al., where they measured them experimentally. (Meena, Niyaz and Gupta, 2023). To model the microcracks using the distributed diode model, the corresponding parameters have been changed accordingly. Microcracks can affect the performance of the solar cell through three types of mechanisms which affect different model parameters. The three possible mechanisms for power loss due to microcracks are (a) Resistive loss mode, (b) Recombinative loss mode, and (c) a combination of both types of loss modes. Also, the orientation of the microcracks plays a critical role in affecting the power of the solar cell (Kajari-Schröder *et al.*, 2011). Different microcrack orientations can affect the solar cell performance differently. So, the three most commonly occurring orientations of microcracks have been studied. Those three microcrack orientations, namely, (a) diagonal to the busbar, (b) perpendicular to the busbar and (c) parallel to the busbar, are considered for each power loss mode.

3.1. Resistive loss mode

The air gap in the cell, due to the microcrack (Fig. 4), hinders the lateral flow of current on the surface, thus increasing the sheet resistance. To model this, the sheet resistance is increased according to the length, width and depth of the microcrack. Only resistive power loss occurs in this mode as the lateral current must pass through higher sheet resistance or flow in an alternate path, increasing the resistance. To model this type of crack, the sheet resistance values are increased for the corresponding sub-cells through which the microcrack passes for the three different microcrack orientations.

3.2. Recombinative loss mode

Microcracks can increase the recombination of charge carriers in solar cells around it. As microcracks are on the surface of the cell, they can increase the recombination around the p-n junction along the microcrack due to the dangling bond created on the open surface. This can happen without the resistive loss mode. For example, if the microcrack is a scratch on the surface, then the air gap is negligible, and so is the resistive loss. However, due to the enhanced recombination on the microcrack site, it will still affect the performance of the solar cell. In order to model the recombination loss in power due to recombination in the p-n junction due to the microcrack, the reverse saturation current density (J_{02}) of the second diode (D_2 ($n_2 = 2$) is taken as the variable as it directly represents the junction recombination (Van Mölken *et al.*, 2012). Also, as reported in the literature, due to material defects in the microcracked location, the R_{sh} corresponding to the sub-cells decreases, thus affecting the output power. These micro-cracks can also enhance another degradation mode, potential induced degradation (PID), around their location, further increasing the recombination and shunting (Dong *et al.*, 2018). The values for changes in J_{02} and R_{sh} are taken from the literature (Van Mölken *et al.*, 2012; Dong *et al.*, 2018; Kumar, Puranik and Gupta, 2023).

3.3. Combination of resistive and recombinative loss mode

Under outdoor operating conditions, recombinative and resistive microcrack modes operate simultaneously (Mohammed Niyaz, Meena and Gupta, 2021). Herein, the resistive and recombinative loss mode may increase in magnitude depending on the external stress conditions promoting power losses. The performance loss in solar cells due to the simultaneous occurrence of both loss mechanisms is under-researched. To simulate the co-occurrence of both modes, combinations of R_{sheet} values with different J_{02} and R_{sh} values are taken for the three microcrack orientations. The results of the simulations have been discussed in the next section.

4. Results and Discussions

Microcracks with three different loss-impacting mechanisms with three different orientations have been modelled using the distributed diode model, and the circuits are simulated using the PSpice circuit simulator.

4.1. Resistive loss mode

Here, the sheet resistance corresponding to the sub-cells along the microcracks is increased, representing the increase in resistance due to the air gap. The loss in maximum power due to higher sheet resistance for the three orientations of cracks is shown in Fig. 6. It is observed that overall, for all three orientations, the power loss is very low (<1%).

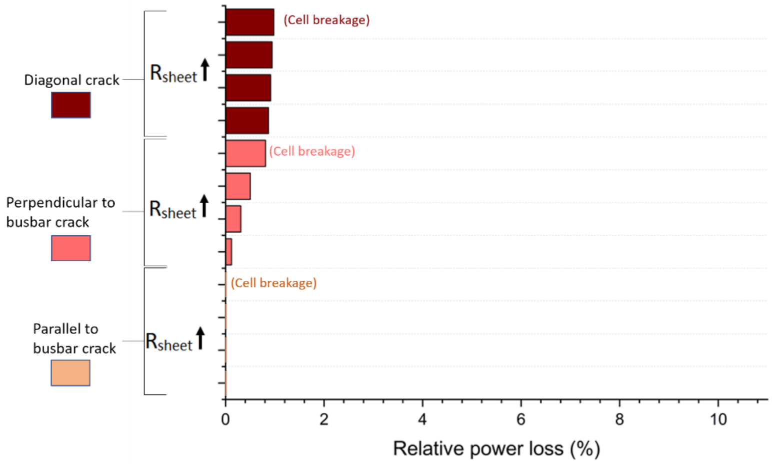

Fig. 6: Power loss due to resistive loss mode for different microcrack orientation

For the diagonal to busbar crack, it is observed that the increase in sheet resistance increases power loss but remains almost constant for higher sheet resistances up to cell breakage. This can be explained as the sheet resistance increases after a certain point, the current finds an alternate path to the nearest finger (Fig. 7), considering that the fingers are not damaged due to the microcrack (Fig. 4). So, after a certain point, increasing the R_{sheet} does not affect the output power of the cell as long as the fingers are not damaged. This also explains the power loss due to the perpendicular to the busbar microcracks, where the microcrack is considered closer to one finger. So, the power output decreases very slightly due to the additional current path introduced, but soon, the lateral current finds the alternative path to the other closest finger; thus, no further decrease in power occurs. For parallel to busbar microcracks, there is no power loss, irrespective of the increase in sheet resistance. This is due to the fact that as long as the finger remains intact, the parallel to busbar cracks do not introduce an additional current path, so the output power is not affected.

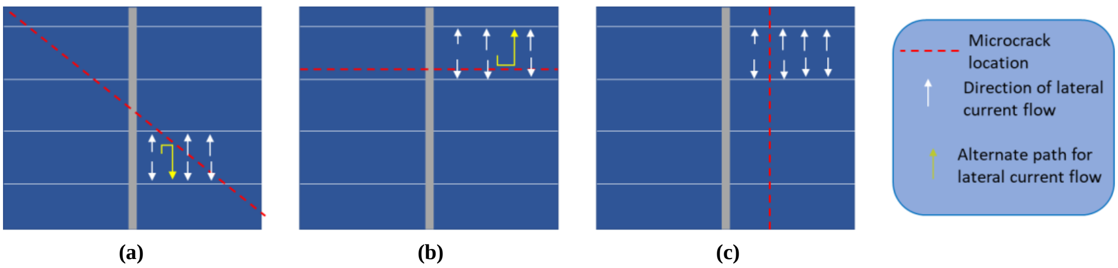

Fig. 7: Lateral current flow directions due to higher sheet resistance for (a) Diagonal, (b) Perpendicular to the busbar, (c) Parallel to the busbar

4.2. Recombinative loss mode

For recombinative loss mode, the relative power loss for different J_{02} values is shown in Fig. 8. The power loss is negligible for low levels of recombination but increases non-linearly with an increase in J_{02}. The slightly higher power loss for the diagonal microcrack can be due to the higher length of the diagonal microcrack.

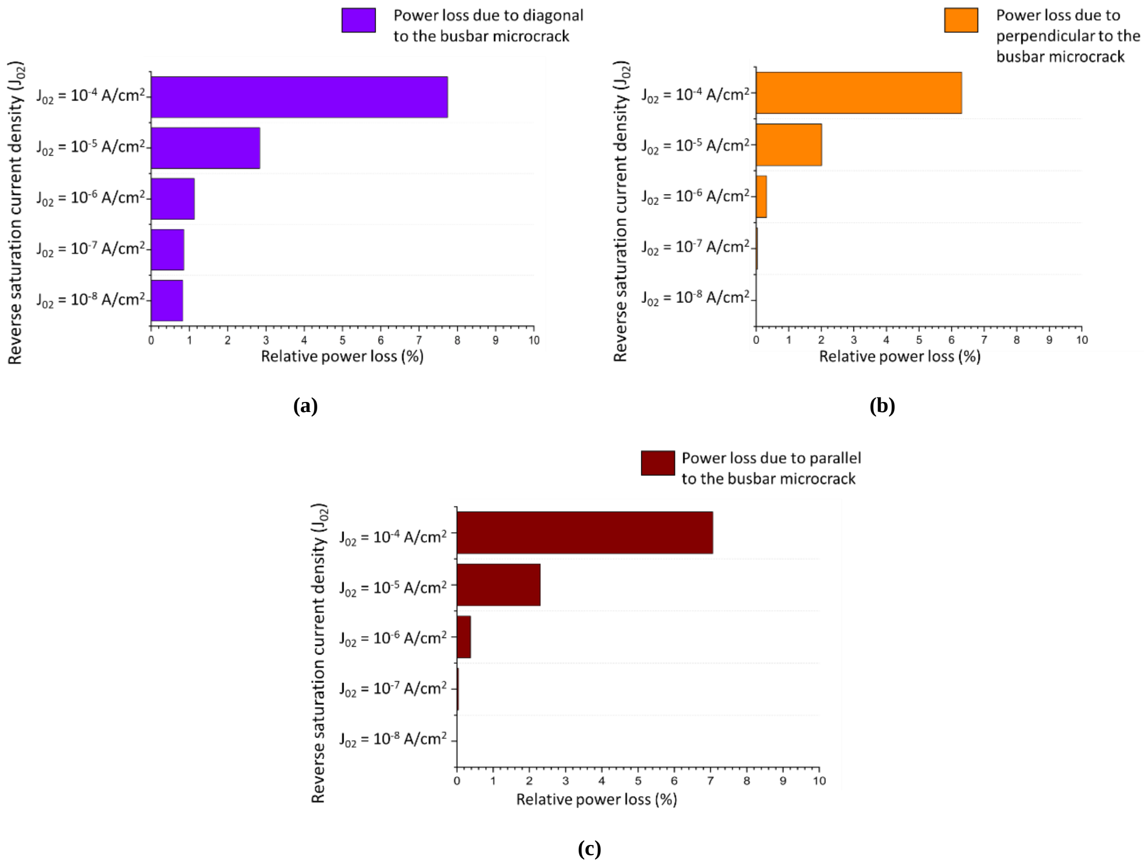

Fig. 8: Power loss due to recombinative loss mode for (a) Diagonal, (b) Perpendicular to the busbar, (c) Parallel to the busbar

The value of J_{02} has been varied from 10^{-8} to 10^{-4} A/cm^2 based on the reported values of change in J_{02} due to recombination losses (Van Mölken *et al.*, 2012; Kumar, Puranik and Gupta, 2023). The recombination around the microcracks can also increase greatly due to possible PID induction around microcracked sites. Maximum power loss of up to 8% is observed due to recombination sites around microcracks for the diagonal to busbar orientation.

4.3. Combination of resistive and recombinative loss mode

The combined effect of both resistive and recombinative losses has been simulated by varying the J_{02} for different R_{sheet} values. The results for diagonal microcracks are shown in Fig. 9(a), 9(b) and 9(c) for different microcrack orientations, respectively.

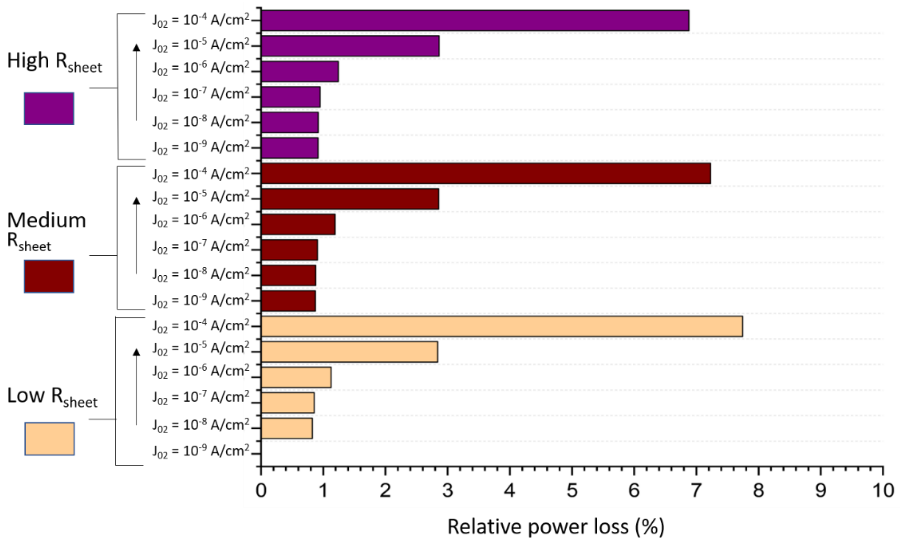

(a)

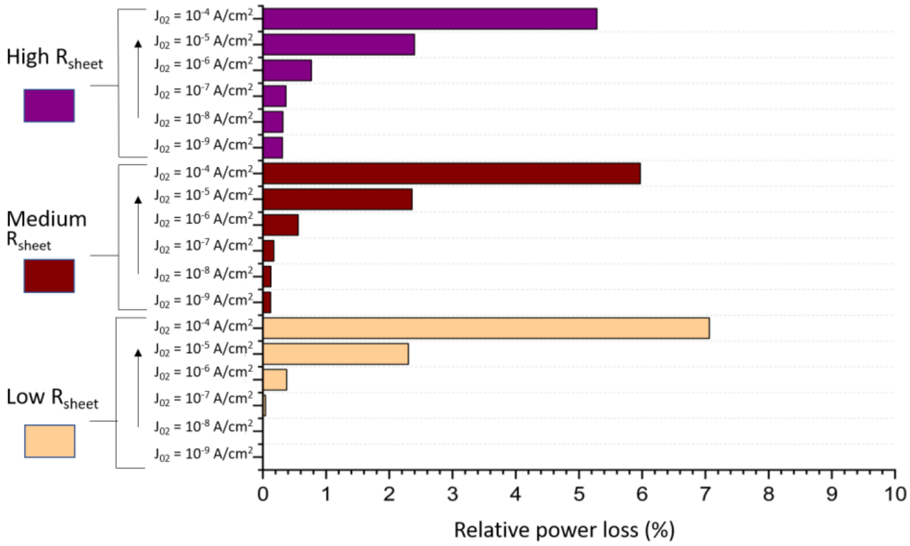

(b)

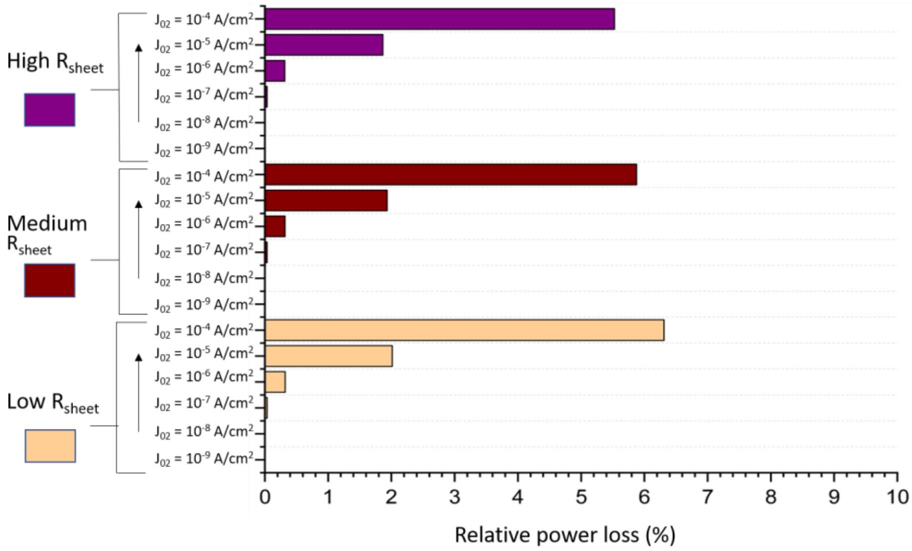

(c)

Fig. 9: Power loss for combination of recombinative and resistive loss mode due to (a) diagonal, (b) perpendicular to the busbar, (c) parallel to the busbar microcrack

It is observed that there are significant power losses due to the combination of both loss modes, the highest loss being for the diagonal microcrack orientation. The power loss for higher J_{02} values decreased with higher R_{sheet} values. The maximum power loss due to the microcrack for all orientations is around 6-8% for the combination of both resistive and recombinative modes. For higher sheet resistance as the lateral current path changes, the recombination of the charge carriers for sub-cells in the path via the microcrack decreases.

5. Conclusion

In this work, the effect of different operating mechanisms of microcrack with three most occurring orientations on the performance of solar cells has been studied using a simulation approach on a distributed diode model. Depending on the electrical parameters affected, the impact of microcracks was classified into resistive mode, recombinative mode and combination of resistive and recombinative mode for power loss. The distributed diode model of solar cells was used to model the spatial impact of power loss incurring modes of microcracks having different orientations. It was observed that for resistive loss mode, power loss increases until a certain threshold value of sheet resistance after which, the power output does not get affected as the lateral flow of current finds an alternate path with less resistance. For recombinative loss mode, the power loss due to recombination in the junction increases non-linearly for high junction recombination. The non-linear increase in power loss is due to the non-linear electrical properties of the diodes, which are mainly affected by the recombination. The combination of both loss-incurring modes affects the output power the most; however, it is not significantly more than the recombinative mode. This spatial impact analysis of microcracks would be helpful to predict the power losses due to microcracks and also their long-term impact on the performance of solar cells.

6. References

Buerhop, C. *et al.* (2012) 'Reliability of IR-imaging of PV-plants under operating conditions', *Solar Energy Materials and Solar Cells*, 107, pp. 154–164. Available at: https://doi.org/10.1016/j.solmat.2012.07.011.

Demant, M. *et al.* (2016) 'Microcracks in Silicon Wafers II: Implications on solar cell characteristics, statistics and physical origin', *IEEE Journal of Photovoltaics*, 6(1), pp. 136–144. Available at: https://doi.org/10.1109/JPHOTOV.2015.2465172.

Dhimish, M. *et al.* (2017) 'Effect of micro cracks on photovoltaic output power: Case study based on real time long term data measurements', *Micro and Nano Letters*, 12(10), pp. 803–807. Available at: https://doi.org/10.1049/mnl.2017.0205.

Dong, N.C. *et al.* (2018) 'The influence of sodium ions decorated micro-cracks on the evolution of potential induced degradation in p-type crystalline silicon solar cells', *Solar Energy*, 174, pp. 1–6. Available at: https://doi.org/10.1016/j.solener.2018.08.082.

International technology Roadmap for photovoltaic (ITRPV) ninth edition, Results 2017." (2018). Available at: http://www.itrpv.net/Reports/Downloads/2018 (Accessed: 20 September 2023).

IRENA Renewable Cost Database (2020) 'Renewable Power Generation Costs in 2020', *International Renewable Energy Agency*, pp. 1–160.

Kajari-Schröder, S. *et al.* (2011) 'Spatial and orientational distribution of cracks in crystalline photovoltaic modules generated by mechanical load tests', *Solar Energy Materials and Solar Cells*, 95(11), pp. 3054–3059. Available at: https://doi.org/10.1016/j.solmat.2011.06.032.

Kasewieter, J. *et al.* (2014) 'Cracks in solar cell metallization leading to module power loss under mechanical loads', *Energy Procedia*, 55, pp. 469–477. Available at: https://doi.org/10.1016/j.egypro.2014.08.011.

Kikelj, M. *et al.* (2021) 'Spatially resolved electrical modelling of cracks and other inhomogeneities in crystalline silicon solar cells', *Progress in Photovoltaics: Research and Applications*, 29(1), pp. 124–133. Available at: https://doi.org/10.1002/pip.3348.

Kumar, R., Puranik, V.E. and Gupta, R. (2023) 'Application of Infrared Thermography for Cell-Level Power Estimation of PID-s Impacted Crystalline Silicon PV Module', *IEEE Journal of Photovoltaics*, 13(1), pp. 141–149. Available at: https://doi.org/10.1109/JPHOTOV.2022.3229485.

Meena, R., Niyaz, H.M. and Gupta, R. (2023) 'Investigation and Differentiation of Degradation Modes Affecting Series Resistance in Photovoltaic Cells and Modules', *IEEE Journal of Photovoltaics*, 13(2), pp.

283–290. Available at: https://doi.org/10.1109/JPHOTOV.2023.3239744.

Mohammed Niyaz, H., Meena, R. and Gupta, R. (2021) 'Impact of cracks on crystalline silicon photovoltaic modules temperature distribution', *Solar Energy*, 225, pp. 148–161. Available at: https://doi.org/10.1016/j.solener.2021.07.038.

Van Mölken, J.I. *et al.* (2012) 'Impact of micro-cracks on the degradation of solar cell performance based on two-diode model parameters', in *Energy Procedia*. Elsevier Ltd, pp. 167–172. Available at: https://doi.org/10.1016/j.egypro.2012.07.046.

Papargyri, L. *et al.* (2020) 'Modelling and experimental investigations of microcracks in crystalline silicon photovoltaics: A review', *Renewable Energy*. Elsevier Ltd, pp. 2387–2408. Available at: https://doi.org/10.1016/j.renene.2019.07.138.

Spataru, S. *et al.* (2015) 'Quantifying solar cell cracks in photovoltaic modules by electroluminescence imaging', in *2015 IEEE 42nd Photovoltaic Specialist Conference, PVSC 2015*. Institute of Electrical and Electronics Engineers Inc. Available at: https://doi.org/10.1109/PVSC.2015.7356124.

Stuart Bowden, C.H. (2019) *PVEducation*. Available at: https://www.pveducation.org/pvcdrom/characterisation/double-diode-model (Accessed: 20 September 2023).

Zekry, A. and Al-Mazroo, A.Y. (1996) 'A distributed SPICE-model of a solar cell', *IEEE Transactions on Electron Devices*, 43(5), pp. 691–700. Available at: https://doi.org/10.1109/16.491244.